AIP | The Journal of Chemical Physics

Deformable homeotropic nematic droplets in a magnetic field

Ronald H. J. Otten and Paul van der Schoot

Citation: J. Chem. Phys. **137**, 154901 (2012); doi: 10.1063/1.4756946
View online: http://dx.doi.org/10.1063/1.4756946
View Table of Contents: http://jcp.aip.org/resource/1/JCPSA6/v137/i15
Published by the American Institute of Physics.

Deformable homeotropic nematic droplets in a magnetic field

Ronald H. J. Otten[1,2,a] and Paul van der Schoot[1,3]
[1]*Theory of Polymers and Soft Matter and Eindhoven Polymer Laboratories, Eindhoven University of Technology, P.O. Box 513, 5600 MB Eindhoven, The Netherlands*
[2]*Dutch Polymer Institute, P.O. Box 902, 5600 AX Eindhoven, The Netherlands*
[3]*Institute for Theoretical Physics, Utrecht University, Leuvenlaan 4, 3584 CE Utrecht, The Netherlands*

(Received 3 November 2011; accepted 18 September 2012; published online 15 October 2012)

We present a Frank-Oseen elasticity theory for the shape and structure of deformable nematic droplets with homeotropic surface anchoring in the presence of a magnetic field. Inspired by recent experimental observations, we focus on the case where the magnetic susceptibility is negative, and find that small drops have a lens shape with a homogeneous director field for any magnetic-field strength, whereas larger drops are spherical and have a radial director field, at least if the magnetic field is weak. For strong magnetic fields the hedgehog configuration transforms into a split-core line defect that, depending on the anchoring strength, can be accompanied by an elongation of the tactoid itself. We present a three-dimensional phase diagram that shows the tactoid shape and director field for a given anchoring strength, tactoid size, and magnetic-field strength. Our findings rationalize the different shapes and structures that recently have been observed experimentally for nematic droplets found in dispersions of gibbsite platelets in two types of solvent. © *2012 American Institute of Physics*. [http://dx.doi.org/10.1063/1.4756946]

I. INTRODUCTION

Nematic droplets consisting of a liquid-crystalline material are often observed in dispersions of sufficiently anisometric colloidal particles under conditions where the isotropic and nematic phase co-exist.[1–7] These so-called tactoids have been investigated quite intensively over the last few decades, not least because of their interesting and sometimes unusual shapes and internal structures and relevance to display technology.[2] These include oblate and prolate droplet shapes with round and sharp edges, and director-field structures involving surface and bulk point defects as well as ring-shaped disclination lines and bipolar twisted "parity-broken" director fields, all depending on the size of the drops and the shape of the colloids.[1,3–9]

Because the shape and structure of tactoids result in effect from a competition among surface, anchoring, and elastic forces, studying them provides quantitative information on material properties of liquid crystals, including the elastic constants, surface tension, and anchoring strength of the director field to the interface between the co-existing isotropic and nematic phases.[3,4,6–12] Tactoids in lyotropic systems are more suitable for this purpose than those in thermotropics because of the extremely low surface free energies in lyotropics.[13–15]

Studies on tactoids in dispersions of *rod-like* colloidal particles such as vanadium pentoxide,[1,3,4] f-actin,[5] tobacco mosaic virus,[16] boehmite,[17] and fd virus,[18] have shown that these drops tend to have a bipolar director field in which the curved field lines run from one virtual surface point defect (boojum) to another on the other side of the drop. The reason for this tendency for bipolar director fields is that rod-like particles for entropic reasons prefer planar alignment of the director to the interface. Theoretically one only expects this to be so if the drops are sufficiently large relative to some length scale set by the elastic and interfacial properties of the nematic drops.[19] Tactoids with uniform director fields have been observed in computer simulations and recently also in dispersions of carbon nanotubes.[6,20,21] The structure of tactoids with planar anchoring conditions have been studied theoretically in great detail.[3–6,8,9,17]

Tactoids of *plate-like* colloids seem to have a very different director field from those of rod-shaped ones, although to date much fewer systems have been studied. The rather intricate stabilization of plate-like colloids is presumably the reason for this.[13,22–24] Tactoids have been observed in dispersions of sterically and charge-stabilized gibbsite platelets.[22,25,30,31] For these systems both uniform and radial director fields have been observed, the latter as a result of the tendency of plate-like particles to align homeotropically to interfaces, again for entropic reasons.[31] The radial director field is characterized by a hedgehog point defect in the center of the drop,[2,25–27] which in fact could also be a small ring defect.[28,29]

Theoretically, much less is known of the structure of this kind of drop, in particular in the presence of an external orienting field, such as a magnetic field. Extensive experimental studies have recently been done on tactoids of gibbsite platelets in the presence of an externally applied magnetic field.[30,31] Two types of system were studied: one where the particles were stabilized sterically and dispersed in bromotoluene, and another in an aqueous solution where the platelets were charge-stabilized. Surprisingly, the type of solvent turned out to cause markedly different behavior. In both solvents the tactoids were observed to exhibit a sharp, Frederiks-like transition from a radial director field with a

[a]Electronic mail: r.h.j.otten@gmail.com.

point defect that stretches ("splits") to a line defect if subjected to a sufficiently strong magnetic field. For the case of the sterically stabilized gibbsite this stretching was followed by an elongation of the drop itself for yet stronger fields, whereas in the aqueous system the drops remained spherical.[30]

In fact, the existence of a split-core line defect was predicted theoretically about a decade ago by Mkaddem and Gartland,[29] indicating that it may be stabilized by an externally applied magnetic field. However, this would only be possible if the nematogens have a negative diamagnetic susceptibility, which is the case for gibbsite. So, this corresponds exactly to the situation that was experimentally investigated,[30] and confirmed that the split-core configuration can be stabilized by the magnetic field.

In this work we present a detailed discussion of a macroscopic theory that was shown in previous work to be able to rationalize the experimental observations on tactoids of gibbsite.[30,31] We stress that the theoretical results presented in these earlier papers were completely aimed at rationalizing very specific experimental results and that these papers contain no discussion at all on how these theoretical results were obtained and how generally valid they are beyond the specific cases. We focus now not on a comparison with experiments but a full analysis of the theory and its ramifications for all types of nematic tactoid characterized by a homeotropic surface anchoring and negative magnetic susceptibility, omitted in Refs. 30 and 31. The current manuscript contains a full analytical characterization of the exact shape of homeotropic drops with a homogeneous director field and the differences in shape and energy with one that can be more directly obtained from cut spheres, the aspect ratio of drops with a split-core defect and the length of this defect.

We have summarized our main results in a series of stability diagrams, making our theory straightforward to apply in practical situations, and we discuss in detail the possible crossover routes between different tactoid structures in the presence of a magnetic field. Our approach is variational and largely based on trial functions for shapes and director fields, but we have been able to solve the problem analytically. We describe how the director-field configuration and the tactoid shape are governed by a competition between the surface tension, anchoring strength, bulk elastic properties of the nematic and the response to the magnetic field.

In agreement with experimental observations, we find that small drops are lens-shaped with a homogeneous director field for any magnetic-field strength and larger drops are spherical with a hedgehog point defect for weak or zero magnetic field. If the magnetic field is strong enough, a split-core line defect in the direction of this field becomes more favorable than the point defect. For even stronger fields, the tactoid itself may, depending on the anchoring strength, stretch to a prolate shape that becomes more spherical again at higher field strengths still. The latter conclusion is a prediction amenable to experimental verification although it does require much stronger magnetic fields than used, e.g., in Refs. 30 and 31. We are also interested in the crossover from one director-field structure to another, so we also examine plausible crossover routes. We find that two plausible routes between uniform and radial director fields are always characterized by a free energy barrier. Intermediates are never stable, implying that even though observed experimentally, these must be non-equilibrium structures caused by the creaming or sedimenting of the tactoids in the gravitational field.

The remainder of this paper is structured as follows. In Sec. II we first present the ingredients of the theory and in Sec. III we discuss drops with a uniform director field. Next, we consider non-uniform director fields in spherical drops in Sec. IV and in non-spherical drops in Sec. V. In Sec. VI we explain our phase diagrams for the optimal tactoid shape and structures and our methodology to obtain them. Next, we discuss the crossover routes from uniform to radial director field in Sec. VII. Finally, we discuss the validity of our model and the results in Sec. VIII.

II. INGREDIENTS OF THE THEORY

We first present the ingredients of our macroscopic Frank-Oseen elasticity theory that enables us to rationalize the experimental observations described in the Introduction.[32] Our free energy $F = F_t + F_a + F_e + F_m$ of a tactoid of volume V consists of four contributions associated with the bare surface tension (subscript t) and surface anchoring (a), the elastic deformation (e), and the magnetic field (m).

1. The surface and anchoring energy $F_t + F_a$ we take of the Rapini-Papoular type,[33]

$$F_t + F_a = \int_A d^2\vec{r}(\gamma + \zeta \sin^2\alpha), \tag{1}$$

where the integration is taken over the entire surface area A of the drop and α is the angle between the surface normal $\vec{q} = \vec{q}(\vec{r})$ and the director field $\vec{n} = \vec{n}(\vec{r})$ at the interface. In Eq. (1) γ denotes the bare surface tension and ζ the surface anchoring, i.e., the anchoring free energy per unit area of the drop interface. As already announced, colloidal platelets for entropic reasons prefer homeotropic alignment of the director field to the interface,[13] implying $\zeta > 0$, which is the case we shall be focusing on. This form of the interfacial energy has been shown to be a very accurate representation for rodlike particles,[6] and we presume it reasonable for disklike ones as well;
2. The Oseen-Frank free energy of elastic deformation reads[32]

$$F_e = \frac{1}{2}\int_V d^3\vec{r}(K_1(\nabla\cdot\vec{n})^2 + K_3(\nabla\times\vec{n})^2), \tag{2}$$

if we ignore twist deformation and contributions from the saddle-splay and splay-bend deformation, where the integration is over the volume V of the drop, and K_1 and K_3 are the splay and bend elastic constant, respectively. Inspired by the experimental observations, we also ignore any contributions from bend deformations,[36] and return to this in the discussion;
3. The magnetic energy of a nematic drop is given by[10]

$$F_m = -\frac{1}{2}\rho\Delta\chi B^2 \int_V d^3\vec{r}(\vec{n}\cdot\vec{e}_x)^2, \tag{3}$$

where we have dropped a term that does not depend on the orientation of the director field,[10] ρ is the particle number density, $\Delta\chi$ the diamagnetic susceptibility anisotropy (dimensions J/T^2), and B the magnitude of the magnetic field that we choose to be in the x-direction described by the unit vector $\vec{e}_x$. As our theory intends to explain the observations on dispersions of gibbsite platelets that have a negative magnetic susceptibility we presume $\Delta\chi < 0$,[25,30,34] so the particles have a tendency to orient their director perpendicular to the magnetic field.

From Eqs. (1), (2), and (3) we deduce that the four free energies scale as $F_t \sim \gamma R^2$, $F_a \sim \zeta R^2$, $F_e \sim K_1 R$, and $F_m \sim \Sigma R^3$, with $\Sigma \equiv -\rho\Delta\chi B^2$ (J/m^3) the strength of the magnetic field, and R a measure of the tactoid size, i.e., the radius in case of a spherical drop. We immediately see that for sufficiently small tactoids the elastic deformation must be dominant, giving rise to a uniform director field irrespective of the magnetic-field strength. On the other hand, for very large drops the magnetic energy becomes dominant, forcing the particles to comply with the orientation imposed by this field.

The relative magnitude of these free-energy scalings provides us with more information in terms of three dimensionless groups that follow naturally from this comparison and that turn out to be important for the remainder of this paper.

1. If we compare both surface terms, we find a dimensionless anchoring strength $\omega \equiv \zeta/\gamma$. For large values of ω the anchoring is dominant over the bare surface tension, indicating a preference to deform the interface over an unfavorable surface anchoring of the director field.
2. Combining elastic with surface or anchoring energies gives a scaled droplet size $\mathfrak{R} \equiv R\gamma/K_1 = R\zeta/K_1\omega$. For small values of $\mathfrak{R}$ and $\mathfrak{R}\omega$ the elastic energy dominates over the surface and anchoring energy, leading to a homogeneous director field at the expense of a deformed droplet and imperfect surface anchoring.
3. Taking the ratio of the magnetic and surface energy gives $\Sigma R/\gamma \equiv \beta^2\mathfrak{R}$, with $\beta^2 \equiv \Sigma K_1/\gamma^2$, which is proportional to B^2. It is a positive quantity for in our case $\Delta\chi < 0$. As we also have the identity $\beta^2 = F_m F_e/F_t^2$, a large value of β^2 means either a dominant magnetic field or dominant elasticity, the director field either adopting a uniform director field or forming a split-core line defect in the direction of the magnetic field.

Clearly, we should simultaneously minimize the free energy F with respect to both shape and director field of a tactoid to find these properties. However, this is a formidable constrained-free boundary-value problem that is most probably impossible to solve analytically, and even hard to solve numerically. Hence, the approach we adopt is to impose three types of director field and three types of tactoid shape inspired by experimentally observed ones, shown in Fig. 1, and then to calculate the combinations of a shape and a director field that have the lowest free energy for given values of our dimensionless parameters ω, $\mathfrak{R}$, and β^2.

III. UNIFORM DROPS

From the scaling argument presented in Sec. II it follows that for sufficiently small tactoids the surface energy and magnetic energy are dominated by the rigidity of the director field, making it uniform. Based on the experimental observations,[25,30,31] we presume the drop to orient such that it minimizes the magnetic energy, so it only has a bare surface and anchoring energy contributing to the free energy F^u, where the superscript u indicates that we are dealing with a uniform director field. To calculate the optimal drop shape, we make use of the so-called Wulff construction, which is exact.[40] This has been worked out for the case of planar anchoring, i.e., $\zeta < 0$ by Prinsen *et al.*,[8] and we here extend it to homeotropic anchoring, so $\zeta > 0$.

Here we only present the main results (see supplementary material).[41] The shape that follows from this construction is completely governed by the dimensionless anchoring strength ω. The aspect ratio a is defined as the ratio of the drop size in the direction of the axis of rotational symmetry and the one perpendicular to it, so it is a number smaller than unity for oblate ellipsoids and larger than unity for prolate ones. We find, as presented before in Ref. 31,

$$a = \begin{cases} \dfrac{1}{1+\omega}, & 0 \le \omega \le 1 \\ \dfrac{1}{2\sqrt{\omega}}, & \omega \ge 1, \end{cases} \tag{4}$$

implying that the larger ω, the smaller a, i.e., the flatter the oblate drop.

The shape of the drop is not only characterized by its aspect ratio, but also by its opening angle, which is defined as the angle that the tangent to the drop at the plane of symmetry makes with that plane. The opening angle α of the Wulff shape satisfies

$$\alpha = \begin{cases} \pi/2, & 0 \le \omega \le 1 \\ -\arctan(-\sqrt{\omega - 1}), & \omega \ge 1. \end{cases} \tag{5}$$

So for $0 \le \omega \le 1$ the rim is smooth, but for $\omega > 1$ it has a sharp edge. The opening angle is shown in Fig. 2.

The expression that we find for the free energy F^u is rather lengthy.[41] An approximate and somewhat simpler shape optimizer may be based on lenses constructed from cut-spheres. We find that, although the shape is different because it always has a sharp rim, contrary to the Wulff shape, the difference in the aspect ratios and in the free energy of both types of lens is very small indeed, less than 0.5%. See Fig. 2 where we compare both shapes.[41] In the limit $\omega \to 0$ we find for both models a spherical droplet with an associated free energy

$$F^u = 4\pi\gamma R^2 + \frac{8}{3}\pi\zeta R^2. \tag{6}$$

From Sec. II it follows that for a sufficiently small spherical drop the zero energy cost associated with the elastic deformation and the magnetic field, outweighs the surface anchoring cost of the uniform field. This argument is valid regardless of the magnetic-field strength. For larger tactoids

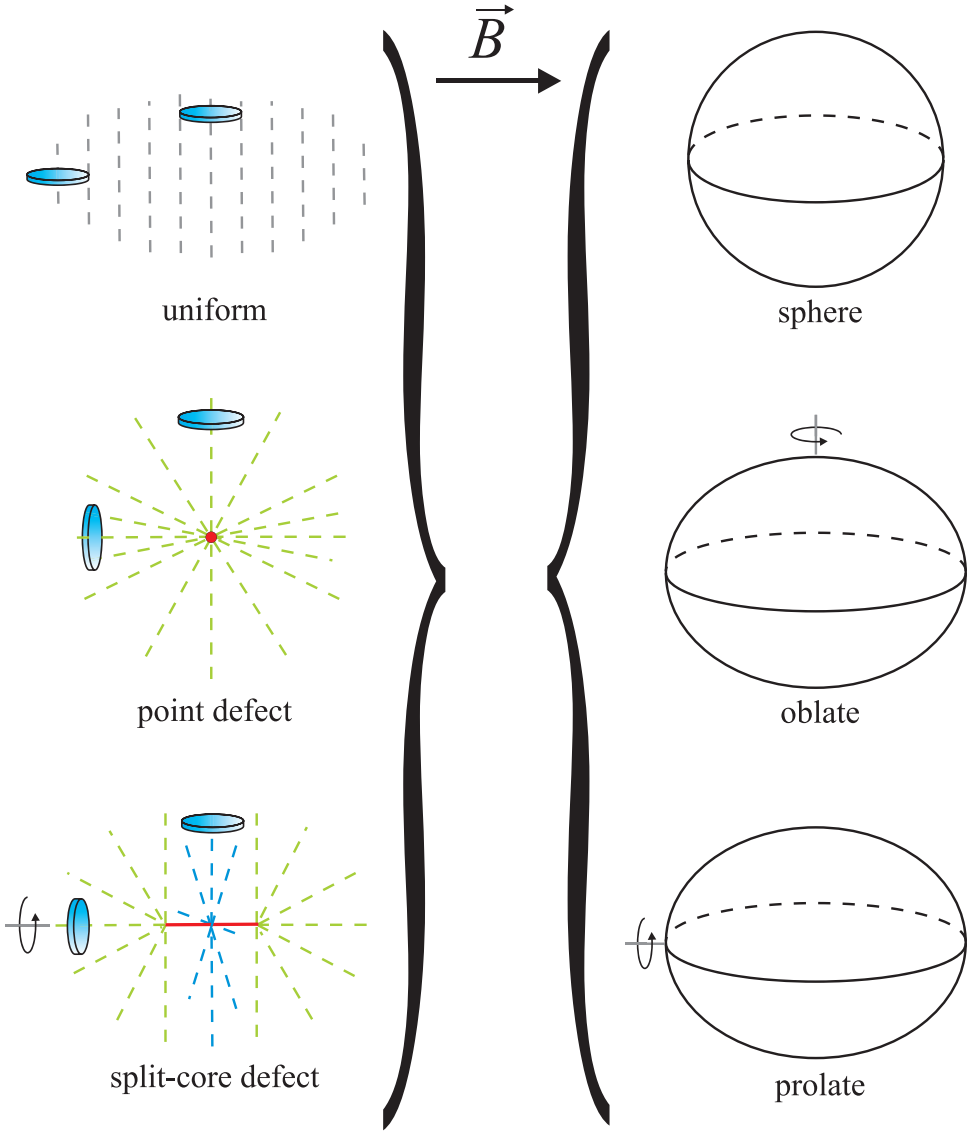

FIG. 1. Based on recent experimental observations on disk-like colloids[25,30,31] we consider three types of director field: a homogeneous field, a three-dimensional radial field, and a two-dimensional radial field around a split-core line defect, capped by a three-dimensional radial field. These three director fields can occur in spherical, oblate, and prolate shapes. The disks are not drawn to scale and merely serve to indicate their orientation.

the anchoring conditions become increasingly important, so the uniform director field can no longer be maintained. In zero field the strong anchoring requirements are fulfilled by a three-dimensional radial director field with a hedgehog point defect in the center of the tactoid, see Fig. 1. In nonzero field this configuration cannot be maintained because of the high magnetic-energy costs. These configurations we discuss in Sec. IV.

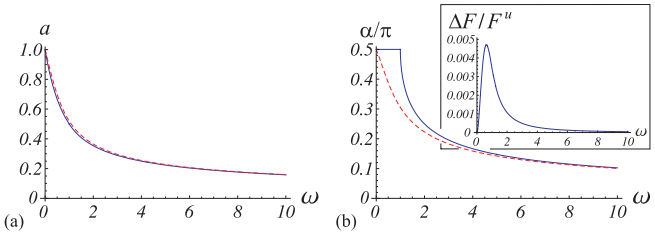

FIG. 2. A comparison of the lens shapes that follow from the Wulff construction (solid lines) and the cut sphere (dashed lines). The aspect ratio a, i.e., the ratio of the short and long axis of the lens shape, is a smoothly decreasing function of the anchoring strength ω (a). The opening angle shows a non-differentiable crossover from a smooth to a sharp boundary (b). Inset: the free-energy difference between the exact Wulff and the cut-sphere shapes ΔF is at most 0.5%.

IV. NON-UNIFORM SPHERICAL DROP

The free energy of a tactoid with non-uniform director field has additional contributions associated with a director-field distortion and the magnetic field. In that case of a three-dimensional radial director field with a hedgehog point defect, the only contribution from the interfacial energy is $F_t^h = 4\pi\gamma R^2$ (superscript h). Using spherical coordinates, the elastic deformation energy and magnetic energy are directly found to be $F_e^h = 8\pi K_1 R$, because $(\nabla\cdot\vec{n})^2 = 4/r^2$, and $F_m^h = \frac{2}{9}\pi\Sigma R^3$ with $\Sigma \equiv -\rho\Delta\chi B^2$ as introduced before. Note that we ignored the free energy associated with the core of the defect.

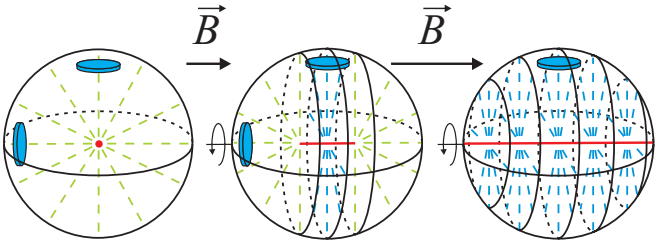

FIG. 3. In order to lower the magnetic energy of the drop in a sufficiently strong magnetic field, the point defect (left) can stretch to a "split-core" line defect in the direction of the magnetic field $\vec{B}$ (middle).[30,31] The defect length increases with the field strength (right).

Hence, the total free energy of the spherical tactoid with radial director field becomes

$$F^h = 4\pi\gamma R^2 + 8\pi K_1 R + \frac{2}{9}\pi\Sigma R^3. \tag{7}$$

In the absence of a magnetic field, $\Sigma = 0$, we can estimate for what droplet size R the hedgehog is energetically more favorable than the uniform field. We see from Eqs. (6) and (7) that $F^h < F^u$ gives $8\pi K_1 R < \frac{8}{3}\pi\zeta R^2$, or $\Re\omega > 3$. Hence, for droplets with a radius larger than $3K_1/\zeta$ anchoring has the upper hand such that the surface-anchoring forces drive the director field into the hedgehog configuration. For lens-shaped droplets, described in Sec. III, we find that our exact but cumbersome expressions for the crossover value can be very well presented by $\Re\omega = 3 + 4\omega/5$ for all values of ω.

For large enough tactoids the hedgehog configuration is more favorable than the homogeneous lens shape but for a sufficiently strong magnetic field it cannot be maintained either because in that case the magnetic energy becomes too large. To comply with the orientation imposed by the magnetic field for a larger fraction of the particles, the tactoid can, besides adopting a uniform director field, split the point defect into two, connected by a line defect of topological charge +1 in the direction of the magnetic field. See Fig. 3.

To model this we presume the director field around this line defect to be radial in two dimensions, and realize that the volume around it has minimal magnetic energy penalty. In the remainder of the tactoid the director field is presumed to have a three-dimensional splay deformation stemming from the original point defect. So, compared to the hedgehog this configuration has a lower magnetic energy penalty, which is even zero for a defect throughout the entire tactoid, but it has a higher elastic deformation energy and nonzero anchoring energy.

Invoking these assumptions on the director field, we separate the computation of the anchoring, elastic, and magnetic energies into a part from the "axis" with the two-dimensional splay deformation, and a part from the ends with the three-dimensional splay deformation. In both parts we presume perfect cylindrical symmetry by invoking cylindrical coordinates. For a given line-defect length L we compute the contributions to the free energy F^{sc} of the split-core defect (superscript *sc*), and we compute the optimal length of the line defect by putting $\partial F^{sc}/\partial L = 0$. The resulting equation is used to eliminate the variable L from the free energy F^{sc}, enabling us to compare the free energy of the split-core configuration with the hedgehog and the drop with uniform director field.[41]

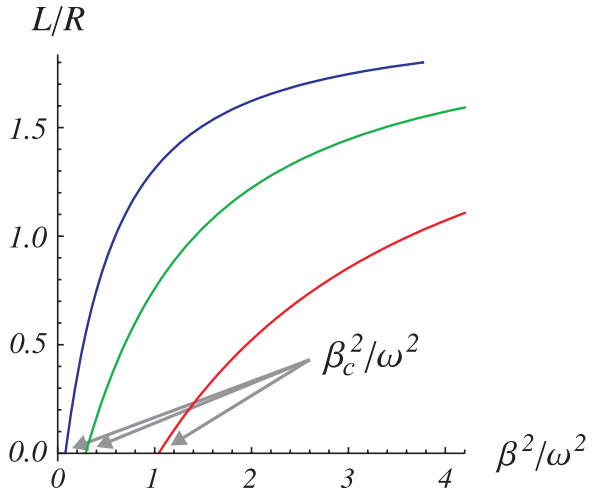

FIG. 4. The length of the line defect L relative to the radius R of the spherical tactoid as a function of the magnetic-field strength β^2/ω^2 as obtained by minimizing the free energy F^{sc} with respect to L. The graphs are for scaled droplet radii $\Re = 5$ (right), 10, and 20 (left). The value for the size of the core b has been chosen to be $b/R = 0.01$.

By comparing Eq. (7) and F^{sc} we find that the crossover from a spherical tactoid with a central hedgehog to one with a split-core disclination requires the magnetic field to be sufficiently strong in order to allow more particles to comply with the orientation imposed by the field. Therefore, it is reminiscent of a Frederiks transition,[42] and the critical magnetic-field strength B_c associated with this transition reads[30]

$$B_c^2 = -\frac{4K_1}{\rho\Delta\chi R^2}\left(\log\left(\frac{b}{R}\right) + 2\right), \tag{8}$$

where b is the diameter of the core of the line defect that we presume to be of the order of the size of the nematogens, because it must be a microscopic length in lyotropic nematics.[38,39] In Ref. 30, Eq. (8) was used to compare the experimental observations and extract values for the splay elastic constant.

At the critical field strength the line defect starts to grow in length, as is shown in Fig. 4. This happens at a dimensionless value of the critical field $\beta_c^2/\omega^2 = \Sigma B_c^2 K_1/\zeta^2$, where B_c is given by Eq. (8), and levels off to an asymptote where $L/R = 2$ for larger field strengths. The expression (8) for B_c is a factor of exactly two thirds smaller than what we found earlier from a cruder model where we presumed perfect surface anchoring and the elongation of the defect to be simultaneously accompanied by a stretch of the drop itself that we presumed to be spherocylindrical.[25] The discrepancy can be explained from the difference in magnetic energy between the two different shapes.

It turns out that spherical drops with a split-core defect elongate for high enough field strengths. This we discuss next.

V. NON-UNIFORM NON-SPHERICAL DROP

A split-core defect induces non-perfect anchoring, which can be alleviated by elongating the drop. To model this we presume the same director field in a prolate drop as for the

spherical drop with a split-core defect. Obviously, the volume of the drop is conserved. The calculation of our free energy of an arbitrary prolate ellipsoid of revolution is rather involved, especially that of the anchoring free energy, so we perform a perturbation calculation near the sphere limit. For the latter we take as a starting point the perfectly spherical drop for which our calculation is exact.[41] This approach is justified by the experimental observation that in practice the deviation from the spherical shape of the observed prolate shape is small.[30]

The perturbation expansion we need to perform in both the shape and the length of the line defect because the latter adjusts to the droplet shape. Hence, one perturbation parameter is the deviation of the aspect ratio from that of the sphere, i.e., unity, and the other is the deviation of the line-defect length from that of the sphere. The calculation is again far from trivial, and here we only outline the concepts.[41]

The free energy F_p^{sc} of the prolate shape (subscript p) we find from the free energy $F^{sc}(L, \varepsilon = 0)$ for the sphere with defect length L and deviation $\varepsilon = 0$ from the aspect ratio of unity of the sphere. The equation for F_p^{sc} reads

$$F_p^{sc}(L_p, \varepsilon) = F^{sc}(L, 0) + \varepsilon \left.\frac{\partial F^{sc}}{\partial \varepsilon}\right|_{\varepsilon=0} + \delta L \left.\frac{\partial F^{sc}}{\partial L}\right|_{\varepsilon=0} + \frac{1}{2}\varepsilon^2 \left.\frac{\partial^2 F^{sc}}{\partial \varepsilon^2}\right|_{\varepsilon=0} + \frac{1}{2}(\delta L)^2 \left.\frac{\partial^2 F^{sc}}{\partial L^2}\right|_{\varepsilon=0} + \varepsilon\, \delta L \left.\frac{\partial^2 F^{sc}}{\partial \varepsilon \partial L}\right|_{\varepsilon=0} + \mathcal{O}(\varepsilon^3, (\delta L)^3), \tag{9}$$

where $L_p = L + \delta L$ is the length of the line defect in the prolate ellipsoid. We optimize F_p^{sc} with respect to the parameters ε and δL, so we put $\partial F_p^{sc}/\partial \delta L = 0$ and $\partial F_p^{sc}/\partial \varepsilon = 0$, giving

$$\left.\frac{\partial F^{sc}}{\partial \varepsilon}\right|_{\varepsilon=0} + \varepsilon \left.\frac{\partial^2 F^{sc}}{\partial \varepsilon^2}\right|_{\varepsilon=0} + \delta L \left.\frac{\partial^2 F^{sc}}{\partial \varepsilon \partial L}\right|_{\varepsilon=0} = 0, \tag{10}$$

$$\left.\frac{\partial F^{sc}}{\partial L}\right|_{\varepsilon=0} + \delta L \left.\frac{\partial^2 F^{sc}}{\partial L^2}\right|_{\varepsilon=0} + \varepsilon \delta L \left.\frac{\partial^2 F^{sc}}{\partial \varepsilon \partial L}\right|_{\varepsilon=0} = 0. \tag{11}$$

The derivatives with respect to L in Eqs. (9), (10), and (11) can be found by direct differentiation; the derivatives with respect to ε we obtain by performing a perturbation of each of the free-energy terms of the spherical tactoid.[41] The procedure gives us L, δL, and ε as a function of $\mathfrak{R}$, β^2, and ω. Representative results are plotted in Fig. 5.

We find that for $\omega > 0$ the aspect ratio for given $\mathfrak{R}$ initially also increases with increasing field strength, starting at a lower critical field $B_{*,\ell}$. Surprisingly, the aspect ratio decreases again to unity for very strong fields at an upper critical field $B_{*,u}$, so the spherical tactoid with a split-core defect re-appears for even larger magnetic-field strengths. See Fig. 5. The reason for this re-entrance behavior is that the length of the line defect affects the balance between the magnetic and anchoring energy. That is to say, the additional free energy of the ellipsoid compared to the sphere with line defect contains mainly a competition between the magnetic energy and the anchoring energy, i.e., the elastic deformation is subdominant. The prolate ellipsoid has a lower anchoring energy throughout the entire tactoid than the sphere, whereas its magnetic energy is larger.

For a weak magnetic field $B < B_{*,\ell}$, the line defect is relatively short and almost all volume of the tactoid is in the ends, which makes the prolate ellipsoid energetically expensive compared to the spherical drop. The larger magnetic energy outweighs the gain in anchoring energy of the elongated drop relative to the spherical one because this is mainly caused in the ends, which is small because of the short line defect. For a larger magnetic field $B > B_{*,\ell}$ the line-defect length is about the size of the tactoid radius and the difference in magnetic energy between the prolate ellipsoid and the sphere becomes even larger than for a smaller value of B. However, this is compensated for by the gain in anchoring energy because of the longer line defect that is mainly due to the better anchoring in the ends. For even stronger magnetic fields $B > B_{*,u}$, there comes a point where the magnetic energy of the prolate drop is too large to be compensated for by the more favorable anchoring than in the sphere, which is now mainly in the axis part. This is because the line defect is larger than half the size of the tactoid.

Finally, as is clear from Fig. 5, the emergence and stretching of the line defect with increasing magnetic-field strength occurs for lower field strengths than the elongation of the tactoid: $B_c < B_{*,\ell}$. The difference between B_c and $B_{*,\ell}$ decreases with increasing values of $\mathfrak{R}$. So, for large values of $\mathfrak{R}$ we see that initially, i.e., for weak magnetic fields, the split-core defect length and the tactoid length increase equally strongly with increasing field strength. This means that for these relatively weak magnetic fields the approximation of a coupled elongation of the line defect and the tactoid, as was

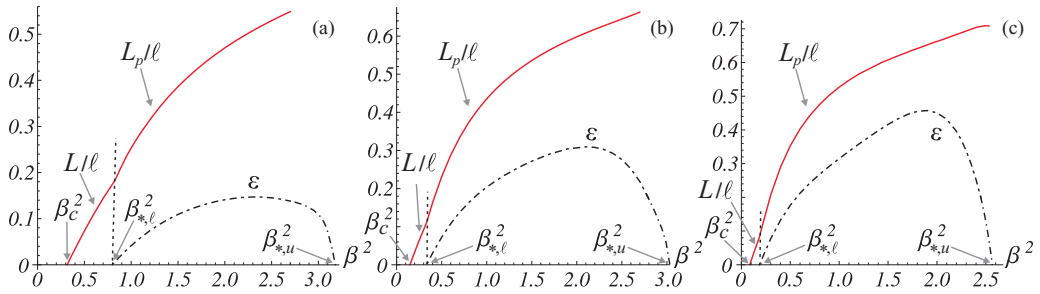

FIG. 5. The length of the line defect in the sphere L and in the prolate drop L_p relative to the tactoid length $\ell = 2R(1+\varepsilon)^{2/3}$ and the increase ε in the aspect ratio $a = 1 + \varepsilon$ as a function of the dimensionless magnetic-field strength β^2 for $\omega = 2$ and $\mathfrak{R} = 10$ (a), 15 (b), and 20 (c). At the critical magnetic-field strength $\beta_c^2 = \Sigma B_c^2 K_1/\gamma^2$ the line defect starts to grow, and for $\beta_{*,\ell}^2 = \Sigma B_{*,\ell}^2 K_1/\gamma^2$ the tactoid itself elongates. The upward deflection to the right of the dashed lines show that beyond $\beta_{*,\ell}^2$ the line defect in the prolate drop is larger than in the equivalent spherical one. At $\beta^2 = \beta_{*,u}^2$ the drop becomes spherical again.

made previously in a much cruder model,[25] is in fact quite reasonable.

In Sec. VI we present the stability diagrams and explain how we compute them.

VI. STABILITY DIAGRAMS

Before considering prolate and oblate tactoid shapes, we first focus on the limit of $\omega \to 0$ where the surface anchoring plays a subdominant role relative to the bare surface tension γ, making the tactoids spherical and the problem independent of γ. This means that the relevant dimensionless groups are given by $\mathfrak{R}\omega = R\zeta/K_1$ and $\beta^2/\omega^2 \equiv -\rho\Delta\chi B^2 K_1/\zeta^2$. The director field is then determined by a balance between the anchoring energy, the elastic deformation energy, and the magnetic energy. The results are shown in Fig. 6. As to be expected from the scaling argument in Sec. II, small tactoids have uniform director field irrespective of the magnetic-field strength, whereas larger tactoids have a hedgehog point defect, provided the magnetic-field strength is small. For larger field strengths the point defect stretches to a split-core line defect to allow more particles to align in the direction imposed by the magnetic field.

The stability diagram of Fig. 6 shows three crossovers between the three director fields. Crossover I from a uniform to radial field is discussed in more detail in Sec. VII and we surmise it is closely related to crossover III from a uniform director field to one with a split-core defect. Finally, transition II from radial director field to the split-core defect is continuous and the required magnetic-field strength B_c is given by Eq. (8). The stability diagram also shows values of constant line-defect length L relative to the sphere radius R. These lines decay with increasing scaled drop size $\mathfrak{R}\omega$ and the limit of $L/R = 2$ gives a vertical asymptote, so it requires an infinitely strong magnetic field. See also Fig. 4.

For nonzero values of ω the surface tension no longer fully dominates the anchoring energy, allowing the drop to deviate from the spherical shape and become oblate or prolate.

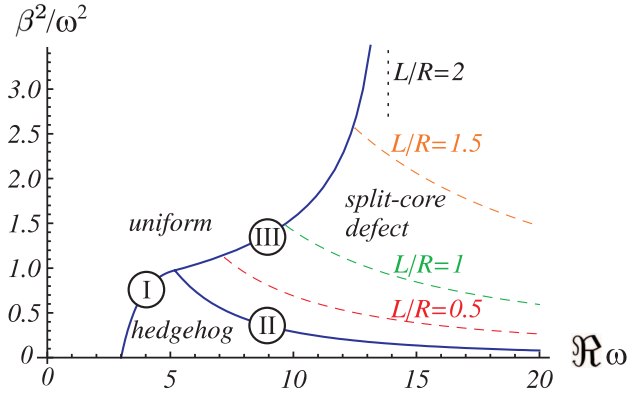

FIG. 6. Stability diagram of nematic drops with homeotropic anchoring in the limit of $\omega \to 0$ where the tactoid is spherical, as a function of $\mathfrak{R}\omega \equiv R\zeta/K_1$ and $\beta^2/\omega^2 \equiv -\rho\Delta\chi B^2 K_1/\zeta^2$ that indicate the drop size and the magnetic-field strength, respectively. The dashed lines show a constant line-defect length L relative to the drop radius R. The vertical asymptote (dotted line) shows the limit of $L = 2R$, i.e., a line defect throughout the entire tactoid. The crossovers I, II, and III are discussed in Secs. VI and VII.

This introduces an additional crossover IV from split-core defect in a spherical drop to one in a prolate drop in the stability diagram, which is continuous. On the boundary of the regime of the prolate drop we have $\varepsilon = \delta L = 0$, so it follows from Eqs. (10) and (11) that to find that boundary it suffices to compute the values of β^2 and $\mathfrak{R}$ that satisfy $\partial F^{sc}/\partial\varepsilon|_{\varepsilon=0} = 0$ and $\partial F^{sc}/\partial L|_{\varepsilon=0} = 0$. The result then gives the lower and upper critical values $B_{*,\ell}$ and $B_{*,u}$ of the magnetic-field strength for a given value of $\mathfrak{R}$, between which the prolate drop is more favorable than the spherical one. In order to find ε and δL in the regime where the prolate drop has the lowest free energy, we need the full equations (10) and (11), plus the added constraint that L is still the optimal solution for the spherical shape, hence $\partial F^{sc}/\partial L|_{\varepsilon=0} = 0$. So for the regime of the prolate drop we have three equations for the three unknowns L, δL, and ε, where a value for the fourth unknown, ω, is selected for every diagram. The lines of constant aspect ratio and constant line-defect length in the stability diagram we then compute by fixing the values of ε and $L_p = L + \delta L$, respectively.

This puts us in a position to compare our free energies and assemble the results in a phase diagram, where the relevant dimensionless groups are now the anchoring strength $\omega \equiv \zeta/\gamma$, drop radius $\mathfrak{R} \equiv R\gamma/K_1$, and magnetic-field strength $\beta^2 \equiv -\rho\Delta\chi B^2 K_1/\gamma^2$. We choose a value of ω and compare each pair of the four director fields with associated shapes for every value of $\mathfrak{R}$, and β. The results of our numerical calculations are summarized in Fig. 7, where take the value of the dimensionless anchoring strength equal to $\omega = 0.25$, 0.5, 1, and 2. The larger the anchoring strength $\omega = \zeta/\gamma$ is, the larger will be the regime of the prolate drop with split-core defect in the stability diagram. The reason is that a higher value of ω means a larger energetic penalty for imperfect surface anchoring, making the prolate drop more favorable than the spherical drop with split-core defect.

The split-core configuration occurs in prolate drops because for all values of the anchoring strength ω that we take, there are values of the dimensionless radius $\mathfrak{R}$ and magnetic-field strength β^2 for which it is the most favorable one of all configurations. For this the tactoid must be sufficiently large to make surface anchoring dominant over elasticity in order to rule out the homogeneous drop, and the magnetic field must be strong enough to force more particles to comply with the preference imposed by this field than in the hedgehog configuration. The magnetic field must be stronger than the lower critical value $B_{*,\ell} > B_c$ to make the elongated drop with split-core defect more favorable than the spherical one, but weaker than the upper critical value $B_{*,u}$. The values of $B_{*,\ell}$ and $B_{*,u}$ that follow from it provides the boundary of the area in the phase diagrams in Fig. 7 where the prolate drop with split core has the lowest free energy.[41]

At this transition for the lower critical value the length L of the line defect is approximately $L \approx R/2$, see Fig. 7. In that figure we plot the lines of constant L/R in the ellipsoid region that have a small downward deflection, implying that the line-defect length in the prolate drop is larger than that in equivalent spherical tactoid. This also follows from Fig. 5. For a given value of $\mathfrak{R}$ the line-defect length increases with increasing magnetic-field strength until it runs throughout the entire tactoid to minimize the magnetic energy cost.

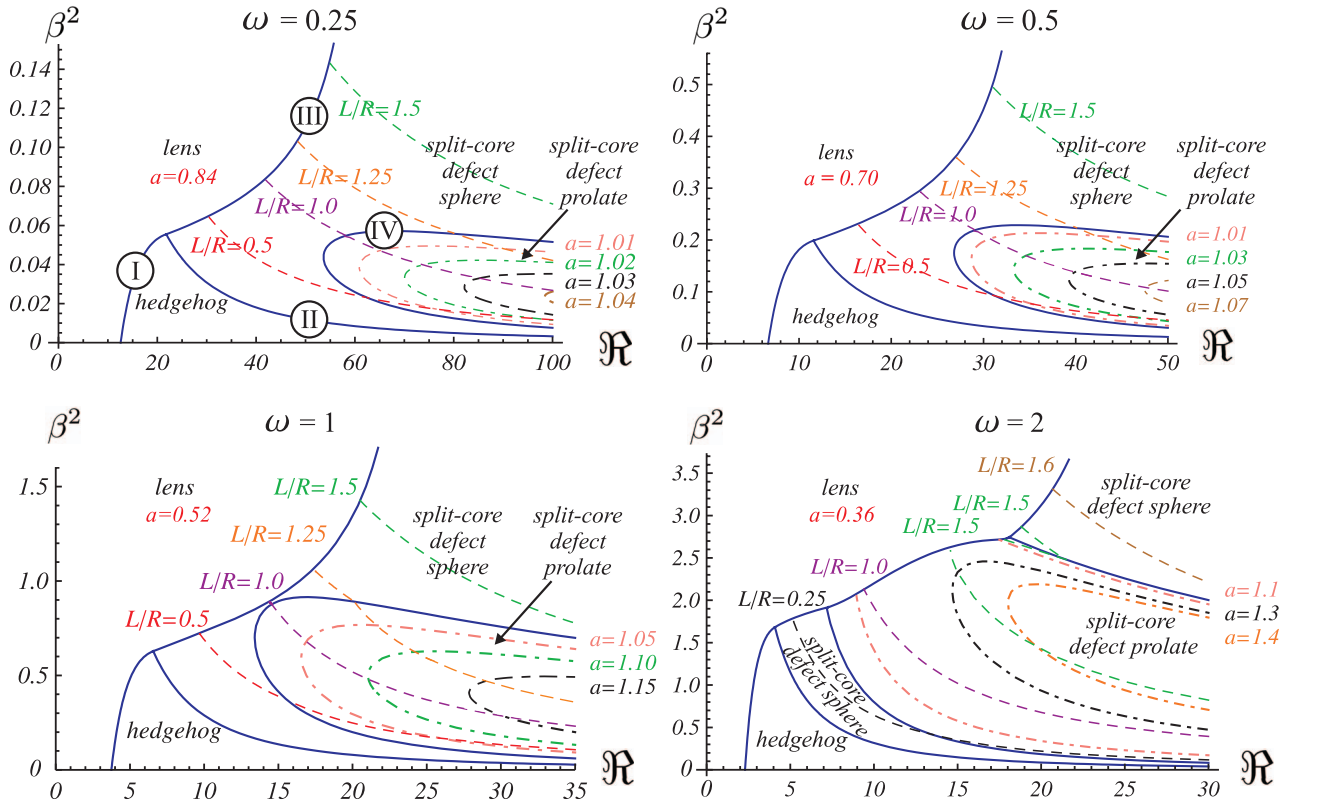

FIG. 7. Stability diagrams of nematic drops with homeotropic anchoring for dimensionless anchoring strength $\omega = 0.25$ (top left), $\omega = 0.5$ (top right), $\omega = 1$ (bottom left), and $\omega = 2$ (right) as a function of the dimensionless radius $\Re \equiv R\gamma/K_1$ and $\beta^2 \equiv -\rho\Delta\chi B^2 K_1/\gamma^2$ that measure the drop size and the magnetic-field strength. The volume is constant for all shapes and equals that of the sphere with radius R. The dashed lines indicate a constant split-core defect length L (or L_p in the prolate drop) relative to R. The dashed-dotted lines show a constant aspect ratio a of the prolate ellipsoid, where $a = 1$ at the crossover from sphere to prolate ellipsoid.[30]

For increasing values of ω, the scale of the horizontal axis decreases, whereas that of the vertical axis increases, but, except for the increasing portion of the parameter space of in which prolate drop is stable, the topology of the diagrams is the same as that of the spherical drop in Fig. 6 for all values of ω. Again, small drops adopt a uniform director field, where the shape is now that of a lens that becomes more oblate for larger values of ω. Larger drops adopt a hedgehog configuration in weak magnetic fields, whereas in stronger magnetic fields the split-core line defect develops.

The stability diagrams of Fig. 7 exhibit four crossover between different director-field configurations and it is *a priori* not obvious how these occur. As advertised above, crossover I from uniform to radial director field will be discussed extensively in Sec. VII and we speculate it is closely related to crossover III from uniform field to split-core defect. Crossovers II from hedgehog point defect to split-core defect within the sphere and IV from this split-core defect within the sphere to one in a prolate drop are, as we have seen, continuous. For transition II we derived Eq. (8) for the critical magnetic field strength that is required, and the lower and upper critical magnetic fields $B_{*,\ell}$ and $B_{*,u}$ for crossover IV were discussed in this section.

Regarding crossover I, recent experiments on tactoids consisting of gibbsite platelets indicate two possible crossover routes and these we discuss in Sec. VII.

VII. UNIFORM TO RADIAL DIRECTOR FIELD

From the stability diagrams of Fig. 7 it is not obvious how the crossover from a uniform to a radial director field occurs. Inspired by experiments on tactoids in dispersions of gibbsite platelets,[30,31] we discuss two possible crossover routes in this section. The first route involves a hedgehog defect that moves away from the center of the drop to infinity, thus crossing over from the hedgehog to the uniform configuration, see Fig. 8. To investigate this route, we compute the free energy of this configuration for an arbitrary location of the defect presuming the drop to be spherical.[41] For the comparison we first take a spherical drop because in that case the surface tension γ is irrelevant. It allows us to compute the free energy of the hedgehog at an arbitrary location using spherical coordinates, given its distance f from the center acting as the continuous variable expressed in units of the drop radius. See Fig. 8. Non-spherical drops are discussed below.

The expression for the total free energy $F^h(f)$ of the hedgehog at an arbitrary position is quite lengthy.[41] If we take the limit $f \to 1$ we find for the free energy of a hedgehog point defect located on the surface of the drop

$$F^h(f=1) = 4\pi\gamma R^2 + 2\pi\zeta R^2 + 4\pi K_1 R + \frac{\pi}{9}\Sigma R^3. \quad (12)$$

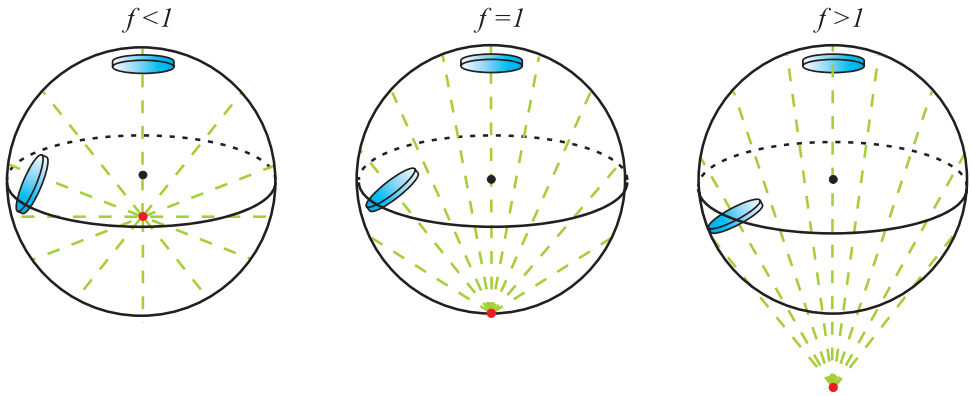

FIG. 8. A possible crossover route from a radial to uniform director field.[31] The hedgehog is located at a distance fR from the center of the tactoid of radius R, so $f > 0$ introduces an additional anchoring cost compared with the central hedgehog ($f = 0$). For $f < 1$ the defect is inside the drop (left), the hedgehog on the boundary follows from putting $f = 1$ (middle), and for $f > 1$ it is virtual, meaning located outside the tactoid (right), with the limit $f \to \infty$ giving a homogeneous director field.

This means that the director field associated with the hedgehog on the surface has an anchoring cost that is absent for the centrally positioned hedgehog, but this is compensated by an elastic deformation and magnetic penalty that are exactly half of those in the central hedgehog.

If we compare the free energy to that of the central hedgehog and the uniform director field, we find that no configuration with the hedgehog defect at a finite distance from the center can be a free-energy minimum, meaning that either the central hedgehog or the uniform field is always more favorable for given values of the parameters $\mathfrak{R}$ and β^2, see also Fig. 9.

Such off-center hedgehog defects have been observed in recent experiments on aqueous dispersions of gibbsite platelets. However, in these experiments it seems that the drop with hedgehog point defect close to the boundary is slightly oblate rather than spherical.[31] Still, if we take an oblate drop by performing a perturbation calculation to find the free energy, we find that there are no values of ω, $\mathfrak{R}$ and β^2 for which the oblate shape has a lower free energy than the central point defect with radial director field *and* the lens shape with a homogeneous field. Hence, in order to make the crossover from the radial to the uniform director field a free-energy maximum has to be overcome that is associated with a configuration with the defect close to the surface of the tactoid. Therefore, we conclude that any hedgehog configuration off-center in general, and the boundary hedgehog in particular, must be an unstable configuration, at least for pure splay fields. We surmise that its occurrence must be caused by the effects of the flow field around the creaming tactoid,[31] and we return to this point in the discussion in Sec. VIII.

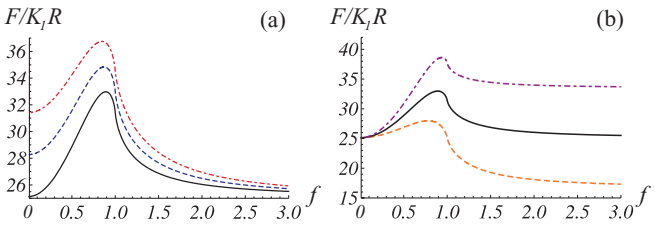

FIG. 9. The free energy F of a spherical drop of radius R with a point defect with radial director field, with K_1 the splay elastic constant, is shown as a function of the distance f between the defect and the center of the drop, expressed in units of R. See also Fig. 8. (a) For $\mathfrak{R}\omega = R\zeta/K_1 = 3$ and from top to bottom $-\rho\Delta\chi B^2 K_1/\zeta^2 = \beta^2/\omega^2 = 1$, 0.5, and 0. (b) For zero magnetic field the three curves show the free energies for $\mathfrak{R}\omega = 2$ (dashed), 3 (solid), and 4 (dotted-dashed). For $\mathfrak{R}\omega = 3$ the free energy of the central defect and the uniform director field ($f \to \infty$) are the same.[31]

A second scenario in crossover I in the phase diagram is by means of the formation of a ring defect that with an increasing radius leads to a homogeneous field inside the tactoid if the ring is much larger than the drop. See also Fig. 10. It turns out that this route has in fact been analyzed by Terentjev,[35] although he did ignore the impact of imperfect anchoring. Terentjev considered a positive diamagnetic susceptibility and a magnetic field parallel to the ring axis, and this symmetry makes the problem equivalent to ours. He showed that in the equal-constant approximation $K_1 = K_3$ a small ring defect can be stable in a magnetic field. For small rings on the scale of the drop the director field is predominantly of the splay type, so the assumption of negligible anchoring energy is reasonable. For larger ring defects this configuration is more favorable than the hedgehog only for large magnetic fields, for which we have seen in Fig. 6 that neither configuration has the lowest free energy. We conclude from Fig. 4 in that paper that an energy barrier has to be overcome for all $\mathfrak{R}^2\beta^2 \lesssim 15$.[35] This means that $\beta^2/\omega^2 \lesssim 15/(\mathfrak{R}\omega)^2$ and if we plot this in Fig. 6, we deduce that this condition is met for a spherical drop for almost any crossover values of $\mathfrak{R}\omega$ and β^2/ω^2, except for a very small interval near the "triple point" where the three director fields have the same free-energy cost. Moreover, if we incorporate the anchoring energy cost, this makes the energy barrier even higher.

So we conclude that only a ring defect that is small on the scale of the tactoid radius can be energetically more favorable than the hedgehog in a spherical drop. For such a small ring defect there is little deviation from the radial director field emanating from the hedgehog point defect, so we chose to omit this configuration in the phase diagram. Hence, neither

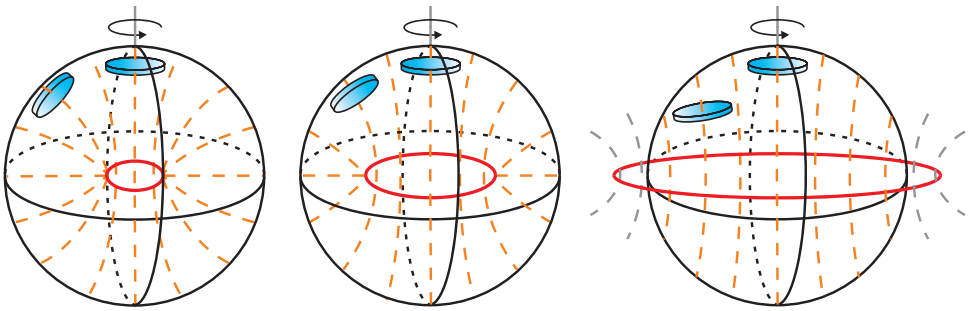

FIG. 10. The second conceivable crossover route from radial to uniform director field. The hedgehog point defect develops into a small ring defect that introduces a bend deformation and an anchoring cost, but this is compensated for by a smaller splay deformation and a lower magnetic energy cost than in the hedgehog configuration. A large ring radius compared to the sphere radius leads to a uniform director field within the drop.

crossover route seems to be a favorable one, and we return to this in the discussion in Sec. VIII.

VIII. CONCLUSIONS AND DISCUSSION

In this work we present a detailed discussion of a macroscopic theory that was shown in previous work to be able to rationalize the experimental observations on tactoids of gibbsite.[30,31] Our approach is variational and largely based on trial functions for shapes and director fields, but we have been able to solve the problem analytically. We describe how the director-field configuration and the tactoid shape are governed by a competition between the surface tension, anchoring strength, bulk elastic properties of the nematic and the response to the magnetic field.

In this paper we have presented a theoretical study of the shape and internal structure of nematic droplets with preference for homeotropic interfacial anchoring of the director field to the surface. If the drops are subject to a magnetic field that imposes a perpendicular orientation of the particles relative to that field, which is the case for a negative diamagnetic susceptibility, this complicates the competition between surface and bulk elastic forces characteristic of isotropic-nematic interfaces. By minimizing the free energies of shapes and director fields in a Frank-Oseen elasticity theory, we have computed the most favorable combination for a given value of the interfacial anchoring strength, the magnetic-field strength, and the tactoid size.

As alluded to above, this work is inspired by recent experimental observations,[30,31] which were explained by the macroscopic theory presented here in detail. The only goal of the theoretical results presented in these earlier papers was to explain the experimental observations, whereas in the present paper we have presented a detailed discussion on how we obtained these theoretical results and how generally valid they are for all types of nematic tactoid with a negative magnetic susceptibility and homeotropic surface anchoring. More specifically, in this work we present a full analytical characterization of the exact shape of homeotropic drops with a uniform director field, the aspect ratio of drops with a split-core defect and the length of this defect. We have summarized our main results in a series of stability diagrams, and we have discussed in detail plausible transition paths between different tactoid structures.

The stability diagrams that we computed confirm the expectation derived from the scaling arguments that in small tactoids the bulk elasticity of the director field is dominant, giving the drop a homogeneous director field, regardless of the magnetic-field strength. The shape associated with this uniform director field is that of a lens, and its aspect ratio, defined as the ratio of small and long axis, decreases with increasing anchoring strength to accommodate with the preferred homeotropic surface anchoring.

For larger tactoids in a weak magnetic field, a hedgehog point defect develops for weak magnetic field because of the predominance of surface anchoring over the bulk elasticity of the director field. As has recently been observed in experiments on tactoids in dispersions of gibbsite plate-like particles, the crossover from a radial to a uniform director field may occur via the formation of a ring defect that increases to infinite radius or via a dislocation of the point defect from the center to the boundary and eventually, to infinity.[30,31] We have shown that a small ring defect may be a stable configuration, whereas a hedgehog defect at a finite distance from the center cannot be a free-energy minimum.

However, in both crossover routes there is an energy barrier that has to be overcome. Substituting typical values into the free energies shows that the height of both energy barriers ranges from hundreds to thousands times the thermal energy k_BT, ruling out the option of completing the crossover spontaneously in a single drop via thermal fluctuations. The energy barriers imply that the transient configurations observed experimentally must be unstable and we surmise that their occurrence must be the result of the flow field in the sedimentation process associated with the phase separation into coexisting isotropic and nematic phase. This conjecture is corroborated by the observation that the boundary defect are always observed on the same (far) side of the tactoids.[30] In fact, flow fields are known to affect director fields in nematic droplets.[37]

For strong enough magnetic fields the hedgehog configuration with radial director field has such a high magnetic energy cost that the point defect stretches to a split-core line defect that allows more particle to comply with the orientation imposed by the magnetic field. A recent paper[30] provided the (to our knowledge) first experimental confirmation of the prediction by Mkaddem and Gartland[29] that a split-core defect can be stabilized by a magnetic field for particles with

a negative diamagnetic susceptibility anisotropy, which is the case for the plate-like gibbsite platelets that were used in the experiments.[30] In this work we have shown how the dominant magnetic field forces the particles to adopt such a split-core configuration and for what values of the drop size and magnetic-field strength it should be stable.

In fact, many more of our theoretical results are borne out by the experiments that were conducted recently. First, a uniform director field was observed for small enough droplets.[30,31] Second, for sufficiently large drops in a weak or absent magnetic field, a hedgehog point defect with radial director field in a spherical drop develops. Third, in the split-core configuration for even stronger fields the length of the line defect increases with increasing magnetic-field strength up to a point were the defect line runs through the entire tactoid. We note that this limiting case requires a very strong field such that the alignment of the isotropic background becomes significant, making it difficult to observe the details of the drop experimentally. Depending on the anchoring strength, the drop itself may stretch to a prolate shape, and this was also observed in experiments on tactoids of sterically stabilized gibbsite. Interestingly, tactoids in dispersion of charge-stabilized gibbsite remained spherical.[30]

We put forward that a difference in the anchoring strength is the cause of different experimental observations in the two types of dispersion. Indeed, by fitting to our theoretical predictions the observed aspect ratio of the drops in the sterically stabilized system and line-defect length in both the sterically stabilized and the charge-stabilized system, we extracted values of $K_1 = 1.0 \pm 0.5 \times 10^{-13}$ N, $\gamma = 2 \pm 1 \times 10^{-8}$ N/m, and $\omega \approx 2$ for the sterically stabilized gibbsite, and $K_1 = 2 \pm 1 \times 10^{-13}$ N and $\zeta = 4 \pm 2 \times 10^{-8}$ N/m for the charge-stabilized gibbsite.[30,31] The latter system exhibits no deviation from the spherical shape, making the analysis independent of the dominant bare surface tension γ and giving $\omega = \zeta/\gamma \to 0$. The values of K_1 are in agreement with earlier results from a much cruder model[25] and with capillary rise experiments for gibbsite platelets in toluene that were sterically stabilized,[13] but the value of the surface tension of $\gamma = 3 \times 10^{-9}$ N/m in that work is much smaller than what we find here. The value $\omega \approx 2$ is required to reach the aspect ratios that were observed recently in the experiments on sterically stabilized gibbsite using bromotoluene,[30] which is significantly larger than the value of approximately $\omega = 0.5$ that was found from the mentioned capillary rise experiments.[13] It should be noted that these experiments are very sensitive to the experimental procedure.[43]

There are two possible caveats of our model. The first is that we neglected the influence of the magnetic field on the material parameters. The second is that except for the configuration with ring defect, we only consider splay deformations of the director field. Although it might appear that the observed director fields exhibit merely a splay deformation, any bend deformation could give a significant contribution because a value of $K_3 \approx 7 \times 10^{-14}$ N has recently been observed for platelets,[34] which would favor a bend deformation over a splay distortion. This has to be compared to the value of $K_1 \approx 1 - 2 \times 10^{-13}$ N that was found recently from the comparison between the experiments and our model.[31] However, it seems unlikely that the incorporation of the bend and/or saddle-splay elastic constant can account for the large discrepancy between the calculated value of the anchoring strength and surface tension that follow from the model, and the value obtained earlier from capillary rise experiments.[13,25]

As already mentioned above, we also neglected the effect of the magnetic field on the material parameters in this work, which may be questionable because of, e.g., the alignment of the background isotropic phase for with increasing field strength. The alignment of the isotropic phase must affect the values of the surface tension and anchoring strength that presumably become smaller due to the alignment. Moreover, the magnetic field increases the nematic order parameter of the nematic phase, which should affect the splay elastic constant K_1 and the anchoring strength ζ. This impact is different for the two parameters because the anchoring strength is proportional to the nematic order parameter and the elastic constant scales with the square of it.[10] The elastic force and surface-anchoring forces compete with the magnetic force against deformation, so an underestimation of K_1 would lead to a too large value of the surface tension. Still, the question remains whether this effect is strong enough to explain the large discrepancy between the quoted values of the surface tension.

ACKNOWLEDGMENTS

The work of R.O. forms part of the research programme of the Dutch Polymer Institute (DPI, Project No. 648). The authors thank Lia Verhoeff and Henk Lekkerkerker for conducting the experiments and many stimulating discussions.

[1] H. Zocher, Zeits. f. Anorg. Chemie **147**, 91 (1925).
[2] P. Drzaic, *Liquid Crystal Dispersions* (World Scientific, Singapore, 1995).
[3] A. V. Kaznacheev, M. M. Bogdanov, and S. A. Taraskin, J. Exp. Theor. Phys. **95**, 57 (2002).
[4] A. V. Kaznacheev, M. M. Bogdanov, and A. S. Sonin, J. Exp. Theor. Phys. **97**, 1159 (2003).
[5] P. W. Oakes, J. Viamontes, and J. X. Tang, Phys. Rev. E **75**, 061902 (2007).
[6] N. Puech, E. Grelet, P. Poulin, C. Blanc, and P. Van der Schoot, Phys. Rev. E **82**, 020702 (2010).
[7] L. Tortora and O. D. Lavrentovich, Proc. Natl. Acad. Sci. U.S.A. **108**, 5163 (2011).
[8] P. Prinsen and P. van der Schoot, Phys. Rev. E **68**, 021701 (2003).
[9] P. Prinsen and P. van der Schoot, Eur. Phys. J. E **13**, 35 (2004).
[10] P. G. de Gennes and J. Prost, *The Physics of Liquid Crystals* (Oxford University Press, 1993).
[11] J. X. Tang and S. Fraden, Liq. Cryst. **19**, 459 (1995).
[12] S. Fraden, A. J. Hurd, R. B. Meyer, M. Cahoon, and D. L. Casper, J. Phys. (Paris), Colloq. **46**, C3–85 (1985).
[13] D. van der Beek, H. Reich, P. van der Schoot, M. Dijkstra, T. Schilling, R. Vink, M. Schmidt, R. van Roij, and H. Lekkerkerker, Phys. Rev. Lett. **97**, 087801 (2006).
[14] W. L. Chen, T. Sato, and A. Teramoto, Macromolecules **29**, 4283 (1996).
[15] W. L. Chen, T. Sato, and A. Teramoto, Macromolecules **31**, 6506 (1998).
[16] J. D. Bernal and I. Fankuchen, J. Gen. Physiol. **25**, 111 (1941).
[17] H. Zocher and C. Török, Kolloid-Z. **170**, 140 (1960).
[18] Z. Dogic and S. Fraden, Philos. Trans. R. Soc. London **359**, 997 (2001).
[19] P. van der Schoot, J. Phys. Chem. B **103**, 8804 (1999).
[20] Y. Trukhina, S. Jungblut, P. van der Schoot, and T. Schilling, J. Chem. Phys. **130**, 164513 (2009).
[21] A. Cuetos and M. Dijkstra, Phys. Rev. Lett. **98**, 095701 (2007).
[22] F. M. van der Kooij and H. N. W. Lekkerkerker, J. Phys. Chem. B **102**, 7829–7832 (1998).
[23] F. M. van der Kooij, K. Kassapidou, and H. N. W. Lekkerkerker, Nature (London) **406**, 868–871 (2000).

[24]A. B. D. Brown, S. M. Clarke, and A. R. Rennie, Langmuir **14**, 3129–3132 (1998).
[25]A. A. Verhoeff, R. H. J. Otten, P. van der Schoot, and H. N. W. Lekkerkerker, J. Phys. Chem. B **113**, 3704–3708 (2009).
[26]A. Kilian, Liq. Cryst. **14**, 1189 (1993).
[27]O. D. Lavrentovich, Liq. Cryst. **24**, 117 (1998).
[28]E. Penzenstadler and H. R. Trebin, J. Phys. (France) **50**, 1027 (1989).
[29]S. Mkaddem and E. C. Gartland, Phys. Rev. E **62**, 6694 (2000).
[30]A. A. Verhoeff, R. H. J. Otten, P. van der Schoot, and H. N. W. Lekkerkerker, J. Chem. Phys. **134**, 044904 (2011).
[31]A. A. Verhoeff, R. H. J. Otten, I. A. Bakelaar, P. van der Schoot, and H. N. W. Lekkerkerker, Langmuir **27**, 116 (2011).
[32]F. C. Frank, Discuss. Faraday Soc. **25**, 19–28 (1958).
[33]A. Rapini and M. Papoular, J. Phys. (Paris), Colloq. **30**, C4–54 (1969).
[34]D. van der Beek *et al.*, Phys. Rev. E **73**, 041402 (2006).
[35]E. M. Terentjev, Phys. Rev. E **51**, 1330 (1995).
[36]In Sec. VII we consider a ring defect that has a director field with both a splay and a bend deformation, but in the parameter range where this configuration is most favorable, it has hardly any bend deformation.
[37]A. Fernandez-Nieves, D. R. Link, M. Marquez, and D. A. Weitz, Phys. Rev. Lett. **98**, 087801 (2007).
[38]R. B. Zasadzinski and J. Meyer, Phys. Rev. Lett. **56**, 636 (1986).
[39]W. Song, I. A. Kinloch, and A. H. Windle, Science **302**, 1363 (2003).
[40]G. Z. Wulff, Z. Kristallogr. **34**, 449 (1901).
[41]See supplementary material at http://dx.doi.org/10.1063/1.4756946 for details of the derivaiton.
[42]V. Frederiks and V. Zolina, Trans. Faraday Soc. **29**, 919 (1933).
[43]A. A. Verhoeff, private communication (October 24, 2011).